Effects of a Reduction in Crystal Thickness on Anger-Camera Performance

Henry D. Royal,* Paul H. Brown,† and Ben C. Claunch

Rhode Island Hospital and the Veterans Administration Hospital, Providence, Rhode Island

The performances of two commercial gamma cameras,‡ with crystals 1.3 and 0.6 cm thick, are compared. Phantom studies simulating clinical conditions showed no significant difference in performance at 140 keV. At 68 keV, the thinner crystal gave marginal improvements in camera performance with phantoms simulating clinical conditions. Frequent use with very low-energy emitters, such as Tl-201, would be needed to justify the expense required to refit the 1.3 cm camera with a 0.6 cm crystal.

J Nucl Med 20: 977–980, 1979

During the course of an evaluation of mobile gamma cameras (*1*), we had the unique opportunity to study the effects of a reduction in crystal thickness (*2*) on the performance of a commercial model.‡ The results of this study are of theoretical interest, comparing observed and predicted changes in performance due to a reduction in crystal thickness. Practically, the results should help physicians who own a camera with a 1.3-cm crystal to decide whether the benefit from refitting the camera with a 0.6-cm crystal would be worth the cost.

MATERIALS AND METHODS

Both cameras were tested at the factory under the supervision of factory representatives who had certified that both were performing optimally. The camera with the 1.3-cm crystal was tested several months before the one with the 0.6-cm crystal. Except for different photomultiplier tubes, the electronics of the newer camera were unchanged. A different set of collimators was used with each camera.

Unless otherwise stated, Polaroid images containing 2,000 cts/cm^2 were obtained at a rate of approximately 10,000 cps with a 20% symmetrical window. The images were identified only by random numbers and were evaluated independently by three experienced nuclear medicine physicians and one physicist. Images were regarded as clearly different only if there was complete agreement to that effect.

Count-rate capability. Curves showing count rate versus activity were determined by placing 122-keV sources (various amounts of Co-57 in 20 ml of saline in a 30-ml glass vial) one meter below an uncollimated, unshielded crystal. The count rate for a total of at least 300,000 counts was obtained for each source. Deadtimes and percentage data loss were determined using Sorenson's model, which assumes a gamma camera to be composed of paralyzable and nonparalyzable components in series (*3*). Details of this deadtime analysis have been reported elsewhere (*1*).

Flood uniformity. Intrinsic flood fields were obtained without a lead collar, using symmetrical windows of 20, 15, 10, and 5% with a Tc-99m "point" source 2 m from the face of the crystal. Extrinsic

* Current address: Div. of Nuclear Medicine, Peter Bent Brigham Hospital, Boston, MA 02115.

† Current address: Nuclear Medicine Service, Veterans Medical Center, Portland, OR 97207.

Received Jan. 4, 1979; revision accepted March 30, 1979.

For reprints contact: Henry D. Royal, Div. of Nuclear Medicine, Beth Israel Hospital, 330 Brookline Ave., Boston, MA 02115.

flood fields were obtained using symmetrical windows of 20, 15, 10, and 5% with a Tc-99m flood source at the face of the high-resolution collimator.

Spatial resolution, intrinsic and extrinsic. Intrinsic spatial resolution was determined as a function of the count rate for Tc-99m using an ultrafine-resolution sextant phantom, with bars of 1.8, 2.1, 2.5, 2.8, 3.2, and 4.0 mm, placed 1 cm from the uncollimated crystal face, and a "point" source located 2 m from the phantom. Extrinsic resolution was determined for two emitters (Tc-99m and Au-195) using either of two bar phantoms (depending on the distance from the collimator) with a Tc-99m flood source and a Au-195 (68 keV) line phantom.‖ All available parallel-hole collimators were used, with and without 7.5 cm of Masonite scattering material. For Tc-99m, the ultrafine sextant bar phantom was used at the face of the collimator, whereas a coarser, quadrant bar phantom (6.4, 4.8, 4.0, and 3.2-mm bars) was used with the scatterer. (The coarser phantom was necessary with the scattering material because the camera then could not resolve the ultrafine structure.) The Au-195 phantom has line spaces of 10, 20, and 30 mm. A 7.5-cm scatterer thickness was chosen to represent a typical maximum depth in clinical studies.

Efficiency. Relative efficiency with Co-57 and Au-195 was determined for each camera at the face of each parallel-hole collimator by recording the time to accumulate 300,000 counts from a Co-57 liver phantom and a Au-195 line phantom, corrected for decay between studies.

RESULTS

Count-rate capability. No difference in count rate capability was noted. Detailed results for the cameras with the 0.6-cm crystal have been reported elsewhere (*1*).

Flood uniformity. No difference in extrinsic or intrinsic flood uniformity was noted by the observers, therefore, the scintiphotos of flood uniformity are not presented here. Results with the 0.6-cm crystal have been reported elsewhere (*1*).

Spatial resolution, intrinsic and extrinsic. The first column of Fig. 1 shows images of the sextant phantom used to determine intrinsic resolution for Tc-99m at a low count rate. Table 1 shows the results for intrinsic resolution taken from the scoring of images. No changes in intrinsic resolution were noted for count rates up to 50,000 cps. Figure 1 also shows images used to determine extrinsic resolution, obtained with the sextant bar phantom at the face of the high-resolution (HR) collimator and with the quandrant bar phantom and 7.5 cm of scatterer for the HR collimator, the general-purpose (GP) collimator, and the high-sensitivity (HS) collimator. Table 1 shows the results of the scoring for extrinsic resolution. Table 1 also includes the manufacturer's published specifications for both cameras (*4,5*). It has been assumed that bar resolution ≈ FWHM divided by 1.8 (*6*).

Figure 2 shows the images used in evaluation of extrinsic resolution for Au-195, with the line phantom‖ at the face of the HR collimator and with scatterer for the HR, GP, and HS collimators. Although there was agreement among the observers that images with the 0.6-cm crystal were superior to those with the 1.3-cm crystal, no further quantitation was attempted because of the coarseness of the phantom. The images are presented for the reader's own evaluation.

Efficiency. Table 2 lists the theoretical intrinsic

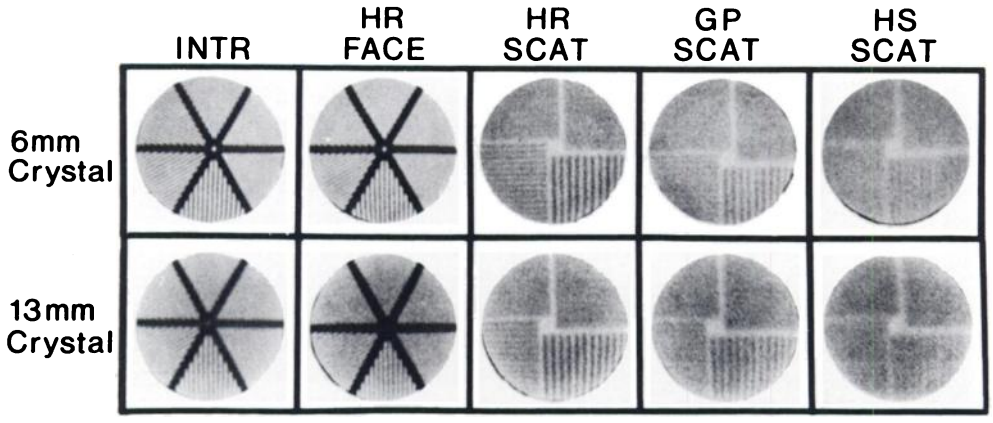

FIG. 1. Comparisons, at 140 keV, between cameras with 0.6- and 1.3-cm crystals. Left-hand pair shows intrinsic spatial resolution; all others extrinsic. Collimators are high-resolution (HR), general-purpose (GP), and high-sensitivity (HS). FACE = source in air, at face of collimator; right-hand six images made through 7.5 cm of Masonite for scattering (SCAT). Sextant bar phantom has lead bar widths of 1.8, 2.1, 2.5, 2.8, 3.2, and 4.0 mm; quadrant phantom has lead bar widths of 3.2, 4.0, 4.8, and 6.4 mm.

TABLE 1. BAR RESOLUTION (mm) AT 140 keV

	1.3-cm crystal		0.6-cm crystal	
	Observed	Specifications* (4)	Observed	Specifications* (5)
Int Res	3.2	3.17	2.5	2.22
HR				
Face	3.2	3.44	2.8	2.50
7.5 cm air		4.75		4.17
7.5 cm scat	4.8		4.8	
GP				
Face	3.2	3.44	2.8	2.50
7.5 cm air		5.28		4.78
7.5 cm scat	6.4		6.4	
HS				
Face	4.0	3.50	3.2	2.56
7.5 cm air		6.44		6.03
7.5 cm scat	> 6.4		6.4	

* Assumes bar resolution = FWHM/1.8.

crystal efficiencies as a function of energy for both crystal thicknesses (7). The change between the 1.3-cm and the 0.6-cm crystal cameras relative to the efficiency of the 1.3-cm crystal camera is also given. Because the theoretical efficiency at 68 keV is 100% even for the thinner crystal, these values were used to compensate for differences in system sensitivity that resulted from factors other than a change in crystal thickness—such as variations in sensitivity among the different collimators and small unintentional variations in window width. The observed change in efficiency at 122 keV between the cameras with 1.3-cm and the 0.6-cm crystals, relative to the 1.3-cm crystal, averaged −15% for all the collimators (range −14% to −16%).

DISCUSSION

With a thinner crystal, the efficiency of light collection increases because each photomultiplier tube subtends a larger angle of the crystal, and the number of photons that interact with the photocathode therefore increases. Since spatial information is affected by Poisson statistics, better collection efficiency results in less noise and therefore better spatial resolution. Energy resolution is also affected by quantum statistics, so that more efficient light collection should also improve energy resolution. Typically, the FWHM for energy resolution decreases from 14% to 12% with a reduction in crystal thickness from 1.3 to 0.6 cm (4,5).

The observed improvement in intrinsic resolution was a fraction of a millimeter at 140 keV. It should be stressed that intrinsic resolution is only one of the factors that determine the total resolution, R_T, of the system as shown by the equation:

$$R_T = \sqrt{R_I^2 + R_C^2 + R_S^2},$$

where R_I = intrinsic resolution, R_C = collimator resolution, and R_S = scatter resolution (8). The only factor that changes with a change in crystal thick-

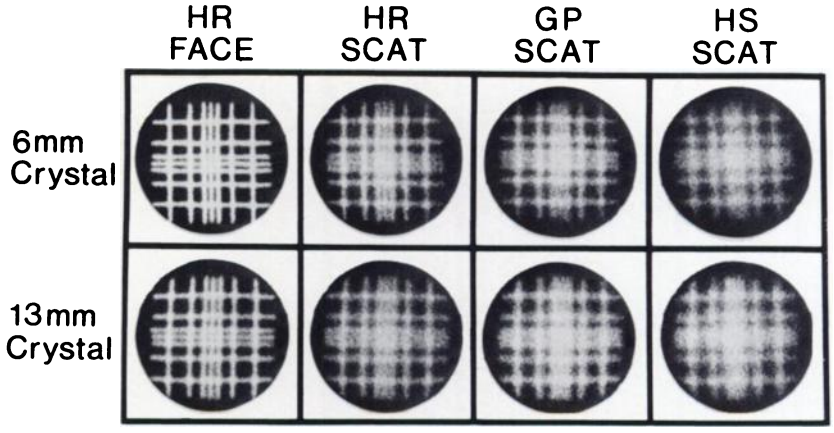

FIG. 2. Comparisons of extrinsic spatial resolution as in Fig. 1, but using Au-195 (68 keV) and phantom with line spacings of 10, 20, and 30 mm.

TABLE 2. THEORETICAL INTRINSIC CRYSTAL EFFICIENCY (%) (7)

Energy (keV)	1.3-cm crystal	0.6-cm crystal	Theoretical difference*
80	100.0	100.0	0.0
100	98.9	96.5	− 2.4
150	90.9	70.7	−22.2
200	71.9	45.2	−36.7

	Observed Change in Efficiency (%)*
68 keV	0
122 keV	−15

* Relative to the efficiency of the 1.3-cm crystal. $Eff._{0.6} - Eff._{1.3}$ $Eff_{1.3} \times 100$.

ness is R_I; therefore, changes in R_T are always less than the change in R_I. In Table 1, the difference in extrinsic resolution at the face of the high-sensitivity collimator between the 0.6-cm and the 1.3-cm crystal cameras was 0.8 mm, whereas the difference in intrinsic resolution between the cameras was 0.7 mm. This deviation from the predicted results (i.e., changes in extrinsic resolution are always less than or equal to changes in intrinsic resolution) is due to the coarseness of the phantom used; this allowed the observers to discriminate only between 3.2-mm and 4.0-mm bar resolution. Note that at 140 keV, under conditions simulating a clinical case (i.e., with 7.5 cm of scatterer) no improvement in resolution was noted.

The thinner crystal's observed 15% loss in efficiency at 122 keV is in agreement with the predicted loss in efficiency (see Table 2). The percentage loss of efficiency increases with rising photon energy. At 140 keV (Tc-99m) the loss in efficiency would be 20%, and at 190 keV (Xe-127, Kr-81m) it approaches 35%. Neither camera has adequate shielding for use above 200 keV.

Camera manufacturers have been willing to trade off losses in sensitivity for improvements in intrinsic resolution because intrinsic resolution has become an important performance parameter for the marketing of a camera. Whether the marginal improvement in resolution—especially in the presence of clinical scatter—is worth the loss in efficiency is dependent on the future development of radiopharmaceuticals. If the use of thallium becomes widespread, the choice of a camera with a 0.6-cm crystal may be advantageous, but if equally promising radiopharmaceuticals with higher energies (Xe-127, Kr-81m) come into routine use, the loss in efficiency will be prohibitive. Currently, for use mainly with Tc-99m, either a 1.3-cm or a 0.6-cm crystal thickness is acceptable, but it would be difficult to justify the considerable cost required to refit a 1.3-cm crystal camera with a 0.6-cm crystal unless it were to be used frequently with very low-energy radiopharmaceuticals.

FOOTNOTES

‡ Searle Low-Energy Mobile Scintillation Camera, Searle Radiographics, Inc., Chicago, IL.

‖ New England Nuclear Corp., Boston, MA.

REFERENCES

1. ROYAL HD, BROWN PH, CLAUNCH BC: Mobile gamma cameras: A comparative evaluation. *Radiology* 128: 229–234, 1978
2. SANO RM, TINKEL JB, LAVALLEE CA, et al: Consequences of crystal thickness reduction on gamma camera resolution and sensitivity. *J Nucl Med* 19: 712–713, 1978 (abst)
3. SORENSON JA: Deadtime characteristics of Anger cameras. *J Nucl Med* 16: 284–288, 1975
4. *Pho/Gamma L. E. M. Scintillation Camera Operation Manual.* Publication No. 710-718830 (Rev. B). Searle Radiographics Inc., Feb., 1977
5. *Pho/Gamma L. E. M. Instrument Specifications,* Model #6475, Ordering Stock #000-77006A, Effective 2/1/78. Searle Radiographics, Inc., Revised August, 1978
6. *Nuclear Medicine, Physics, Instrumentation, and Agents.* Rollo FD, ed: St. Louis, C. V. Mosby, 1977, p 263
7. ANGER HO, DAVIS, DH: Gamma ray detection efficiency and image resolution in sodium iodide. *Rev Sci Instrum* 35: 693–697, 1964
8. BROOKEMAN VA: Component resolution indices for scintillation camera systems. *J Nucl Med* 16: 228–230, 1975